Stepper based maskless microlithography using a liquid crystal display for massively parallel direct-write of binary and multilevel microstructures

Melanie M Kessels, Marwa El Bouz, Robin Pagan, Kevin Heggarty

Stepper based maskless microlithography using a liquid crystal display for massively parallel direct-write of binary and multilevel microstructures

M. M. Kessels [(a)], M. El Bouz [(a)], R. Pagan [(b)] and K. Heggarty [(a)]

(a) GET/ENST Bretagne

Technopôle Brest Iroise, CS 83818, 29238 Brest Cedex 3 (France)

Phone: +33 (0)2290-01031 - Fax: +33 (0)2290-01025

(b) MIVA Technologies GmbH

Benzstr. 17, Business Park Schonaich, 71101 Schonaich (Germany)

Phone: +49 (0) 7031-75600 - Fax: +49 (0) 7031-756030

Melanie.Kessels@enst-bretagne.fr

R.Pagan@mivatec.com

Kevin.Heggarty@enst-bretagne.fr

Abstract A versatile photolithographic photoplotter based on a standard photoreduction stepper where the reticle is replaced by a commercial liquid crystal microdisplay is reported. The microdisplay module is designed as a drop-in replacement allowing the photoplotter to be simply and quickly converted into a standard stepper making it an extremely versatile, low cost R&D tool. Binary and multilevel plotting are demonstrated with plot rates of several Mpixels/s and 1 micron feature sizes into standard industrial photoresists. The limitations on plot rate and resolution are presented and techniques for overcoming them discussed.

Keywords lithography - real-time imaging - liquid crystals - spatial light modulators - micro-optics - optical fabrication

1 Introduction

In recent years, substantial research engineering effort has been directed towards the fabrication of arbitrarily shaped 3D-microstructures because of their broad field of applications in, for instance, the micro-optics, nanotechnology and semiconductor industries [1–6].

These 3D-microstructures are generally fabricated either using multi-step photolithography with standard binary masks (see for example [1]), by gray-scale photolithograhy with coded gray-tone masks [2] or by direct-writing (laser beam [3], x-ray [4], electron beam [5] or ion beam [6]). The first and second methods have the advantage of low cost mass production. Mask fabrication is however a lengthy process and expensive for prototype production. For example, the cost of a set of masks for producing a chip can exceed $ 2 million [7, 8]. Moreover, in most cases, masks present little design flexibility, *i.e.*, once a design has been made on a mask, it cannot be changed unless a new set of masks is

made. Direct writing, on the other hand, is a much more rapid technique for producing small numbers of prototype 3D-microstructures: a laser spot (for example) exposes a pattern in a thin photosensitive layer with technical simplicity and produces high quality structures [3]. Its main disadvantage is that is unsuited to mass production because of the tradeoff between resolution and write time: for high resolution structures the writing-spot diameter must be small but this results in only small areas being written at a time so the overall process is slow. Once a master structure has been made replication techniques [9, 10] can in some cases be used to mass produce relief structures quickly and cheaply. The prototyping remains however slow and hence expensive.

Recently new photolithographic techniques based on a real-time reconfigurable masks have been proposed. This real-time mask is usually either a liquid crystal display (LCD) or a digital micromirror device(DMD) used as a spatial light modulator (SLM) to control system exposure [11–13]. The displayed images can be modified on the SLM in real time. These techniques combine the advantages of a programmable digital LCD or DMD system and a projection photolithography system. Conventional photolithography is greatly simplified as a single LCD or DMD mask can replace a set of conventional masks. For example, the alignment between different levels of masks in conventional photolithography is no longer necessary if the LCD or DMD mask is used because the SLM can display successively different images corresponding to different masks without moving the substrate or the SLM, only the images displayed on the SLM change. The 3D microstructure design can be adjusted rapidly because no mask fabrication is required, only different data files need be generated and then displayed on the SLM.

These SLM based photoplotters present several other important advantages. First production time is shorter than with conventional direct writing techniques for fabricating 3D-microstructures because many (up to a million or more) modulated beams, corresponding

to SLM pixels, simultaneously illuminate the photoresist, hence the term *massively parallel photoplotting*. Secondly, because of this increased speed, short, custom production runs can be performed for low cost. Finally, this technique can also constitute a powerful tool for fabricating photolithographic masks compared to the generally slower and more expensive single write-beam techniques, particularly in the case of low to medium resolution masks [11–13].

Unfortunately putting this basic idea to practical use is often more difficult and expensive than it at first seems. To obtain a competitive performance in terms of structure resolution and plot area, high quality, low distortion reduction optics are required along with a high uniformity SLM illumination system and high resolution (nm precision) XY tables to hold and position the photoresist coated substrate. This often results in practice in a relatively expensive machine.

We present here a photolithographic prototype photoplotter based on a standard photolithographic stepper where we replace the reticle with a LCD screen to directly produce the reduced pattern on the photoresist. Such steppers are readily available or already widely installed and highly optimised for high resolution and large area photoplotting. Compared to SLM based photoplotters that are built from scratch, our system has the advantages of an existing high-performance professional lithographic stepper: reduction lens, autofocus, high precision XY tables, etc. The other major advantage is that the LCD module is designed as a "drop-in" reticle so that the system can be converted from stepper to direct-write photoplotter and back again very simply and quickly. This opens the possibility of using the system in photoplotter mode to write conventional photomasks and then using these masks in stepper mode for longer production runs once the prototype design has been perfected. The overall system is thus extremely versatile and particularly adapted to prototyping or custom production work.

2 Photoplotter design

2.1 Basic principle of massively parallel photoplotting

The prototype parallel photoplotter is essentially built of an SLM, projection lens and a XY table. The basic photoplotter schema is shown in figure 1. A light source is used to illuminate an SLM and the pattern displayed on the SLM is imaged onto the substrate by the projection lens. The data content of a typical plot is usually much greater than the number of pixels on an SLM so a block plotting technique is generally used. Once the first SLM pattern has been exposed, the illumination is blanked out, the XY table on which the substrate is placed moves, the next image block is sent to the SLM, the illumination system unblacked and so on until all of the data has been plotted.

2.2 Overall system design

The prototype parallel photoplotter we have built is based on a GCA 4800DSW photorepeater with a 5 times reduction factor lens. Although more modern photolithographic steppers and photorepeaters offer a higher performance, as is described below, several features of this photorepeater (and also of similar photorepeaters) make it particularly adapted to use with currently available, low cost standard LCD SLMs. As is also shown below, steppers/photorepeaters of this generation have a very respectable performance even by today's standards and especially a high performance/cost ratio. The GCA photorepeater converted into the prototype photoplotter is shown in figure 2. Figure 3 shows the drop-in SLM module at the top of the reduction column. The advantages and the features of the components of this prototype are described in detail below.

2.3 Illumination System

The illumination system is an important component of all photolithographic systems. Here the light source is a mercury arc lamp giving a power of 7.5 mW/cm^2 over 10×10 cm^2 reticle area with a very high degree of uniformity: ±1% across the reticle area. At present only a small part of this area is used because of the small size of currently available SLMs with the required pixel size. As display technology progresses this large area and uniformity will allow us to use a larger, higher pixel count screen than our current screen without having to change the illumination system. The fact that the screen only uses the central reticle area also improves the resolution performance slightly since the performance of the projection lens is greater near the centre.

We chose an illumination wavelength of 436 nm (g-line) to avoid absorption in the SLM and because of the availability of high sensitivity photoresists for both binary and multilevel work at this wavelength. The use of wavelengths below about 400 nm is problematic when standard LCD are used as the contrast drops (both polarisers and modulator) and the LC molecules can be damaged by high optical powers at such wavelengths. Mercury arc lamps cannot be directly modulated so a electro-mechanical shutter is used to illuminate the LCD screen only when a valid image is present.

2.4 LCD Screen

Driven by the display industry, the characteristics of liquid crystals and LCDs have been investigated extensively during last decades. The technologies for manufacturing LCDs are so developed that high-performance and high-resolution LCD panels have become standard "off-the-shelf" inexpensive components that can be used as photomasks for real-time photolithography [11].

The LCD used in our system is a 600x800 pixels liquid crystal spatial light modulator

(SLM) from TL Electronic GmbH [14] (based on a *Sony/Epson* panel). It is positioned using a specially adapted mount on the top of the reduction column with the required polarisers such that the LC plane is in the same optical plane as a standard photolithographic reticle. The pixel pitch is square, 33 μm with a rectangular transparent area in the centre (more details in section 2.8). The screen is a monochrome device with grey level bitmap images coded on 8 bits, theoretically giving up to 256 grey levels.

The refresh rate of the SLM limits the maximum possible plot rate. The photoplotter operates at the upper limit of refresh rate with in practice a minimum delay between successive images of roughly 20 ms: a typical limit for standard nematic LCD like the one used here. Tests with delays down to 10 ms have produced an unacceptable loss in contrast and some partial image loss. More modern SLMs, based on FLC, LCOS or MEMs technology have much faster refresh rates, often of an order or magnitude or more (details in section 4.1). For our current work the plot rate is not a critical parameter for this prototype since the plot rate advantage gained by the massively parallel nature of the SLM means plot rates are already highly respectable.

The PC graphics card is connected to the PC monitor and the SLM via a replicator which allows us to simultaneously display images on the photoplotter SLM and to verify them visually on the ordinary monitor.

2.5 Reduction Column

The highly optimised photoreduction lens is the core component of the projection system and its imaging quality directly influences the plotted characteristics of the patterns in the photoresist [12]. Our reduction lens is a ZEISS 5x with a numerical aperture of 0.30 giving a 1 μm resolution, over a potential 16×16 mm^2 writing field with a total distortion of less than 80 nm across this field. This lens can therefore easily resolve the central

transparent area as well as the opaque inter-pixel space of the separate SLM pixels whose exposed area at the photoresist level is approximately 5×3 μm^2 on a 6.6 μm pitch.

2.6 XY Tables

The substrate is held on XY table with a vacuum chuck. The XY tables included in the GCA photorepeater cover a total range of 15×15 cm^2 using DC motors. To obtain the required accuracy the tables incorporate electromagnetic tips, the DC motors giving the long range movement and voice coil motors giving the short range precise positioning using feedback from a laser based interferometric position detection system with a resolution of 40 nm.

2.7 Electronics and software

Our prototype is based on a GCA stepper built using mainly 1990s technology. As indicated in the previous section, the optics, mechanics and electronics still offer a very acceptable performance so there was no need to change them. On the other hand the original software and the computer hardware (PDP11) is obsolete. We therefore chose to completely change the plotting module of the photoplotter software but to keep the same electronics interface because we need the original control electronics. We used a standard PC with a card from H&L Associates [15] added to directly control the stepper electronics. We chose to work the Linux operating system because of the ease of manipulation of large amounts of memory (plot data) and the ease of access to low level graphics routines bypassing the graphical user interface. A driver to make the interface between the kernel and the stepper electronics was designed using WinDriver Linux from KRFTech [16].

The new software to control and synchronise the image display on the SLM, the XY table, the position detection, the autofocus and the shutter was written by ENST in

collaboration with MIVA Technologies GmbH [17]. It is important that the photoplotter accepts the different file formats used in the photoplotting industries in general. Since the SLM is pixelised, the internal data representation is fundamentally bitmap however software has been written to enable the photoplotter to accept vectorial image formats (Gerber and GDSII, DXF via translators). The photoplotter converts these formats into an internal Run Length Encoded (RLE) format. It can take this internal RLE format, read it and put the image in the PC RAM as a pixmap. This is then used by the image display software. As a result the photoplotter can plot binary and grey-level images with bitmap formats (PGM, TIF, PCX, BMP, ...) or binary plot data in vector formats (RLE directly and Gerber, DXF, GDSII, PostScript, ... after translation).

2.8 Image display

The limited number of pixels and the less than 100% fill factor of the SLM along with the requirement that the same hardware should be used to plot large binary 2D structures and multilevel 3D structures have led to some more sophisticated plotting techniques being developed. The corresponding software was written to correctly cut and display the image to be plotted into screen-sized blocks to be sent to the SLM. The basic principles and reasons for these techniques which we term *block plotting*, *super-resolution*, *step-and-repeat* and *multilevel plot* will now be described briefly.

- ***Block Plotting Technique:*** If the plot data is large it cannot be plotted with one SLM exposure. It has to be plotted by a block-by-block technique. We extract and plot a part of the overall plot data, called a *block image* whose size equals the SLM size. Then the stages are moved to the next block position, a new image displayed and so on until the whole pattern has been exposed (see figure 4). In this way the total plot size is limited only by the XY table range: 15×15 cm^2 rather than the

SLM size.

- ***Super-Resolution (SR) Technique:*** Due to the less than 100% fill factor of SLM pixels and the high resolution of the reduction lens, the surface etched in the photoresist is not flat: the opaque inter-pixel gap (corresponding to insulating tracks, transistors for the LCD active matrix, ...) is unexposed during the illumination. After development, this area is unetched in the photoresist while the transparent pixel centre, exposed during the illumination, is etched down to the substrate after development. Figure 5 shows such a view of a part of the SLM pixel array exposed in the photoresist.

  In order to resolve this problem we have developed a so-called "super-resolution" technique. Data are plotted by displaying several successive images onto the SLM and performing very small translations, by distances that are a fraction (*e.g.* 1/6 th) of the pixel pitch, of the XY tables between each exposure. This effectively fills in the unexposed areas by overlapping the active areas of the different images sent to the SLM. This "super-resolution" (SR) is performed in both the X and Y directions. We generally use a factor 6 super-resolution in both directions giving 36 successive exposures which also eliminate the "staircase" pixelisation effect on diagonal or curved plot patterns. Comparison between patterns etched in photoresist with and without the SR technique is shown on figure 6.

- ***Step-and-Repeat:*** To reduce plot data file size, the software also allows for any image to be repeated using a "step-and-repeat" technique: the pattern is plotted, the stages move and the same pattern is replotted alongside on a regular matrix. This feature is particularly useful for plotting structures such as lenslet arrays or Fourier plane computer generated holograms.

- ***Multilevel Plot:*** Etching 3D data with several different etch depths is done by exposing the photoresist for different lengths of time, the deeper levels being exposed longer than the more superficial levels. This type of multilevel plot could also be performed using the grey levels of the SLM: the lower the grey level in the data image (closer to 0 level), the darker the SLM pixel and the less exposed in the photoresist. However with many SLMs and in particular with the SLM we use, the grey levels are designed for image display and therefore adapted to the human eye so are difficult to control photometrically. As a result we decided to work with exposure time and successive binary images.

  To simplify and increase the speed of the operation, rather than separating the grey level image into a series of binary images, only one grey level bitmap (coded on 8 bits, so giving up to 256 grey levels) is sent to the SLM and the video palette changing routines of the video card are used to control how these images appear as full contrast black and white images on the SLM. Changing the palette is a much simpler and quicker operation than rewriting a whole SLM image, the appearance of the image displayed on the SLM changes in one video cycle so blanking with the mechanical shutter between the different binary versions of the grey level image is not required. This produces a significant increase in overall plot rate: the limiting factor is the relatively fast SLM refresh rate and not that of the slower mechanical shutter. The exposure dose for each level is determined from a look up table (LUT) which is obtained from a calibration of the photoresist's photochemical response. Once this is calibrated it becomes possible to "sculpt" photoresist almost at will to fabricate a very wide variety of 3D shapes. (see section 3.3).

Including all of these techniques, the overall architecture of the control software is therefore as described below. Figure 4 indicates schematically how the different pixels of

the plot data are assembled into data images sent to the SLM.

- Initialisation: read plot data file (see section 2.7 for formats), convert to bitmap, calculate the number of image blocks.
- Image block loop (α, β, γ, ...)
  - Super-resolution loop (A, B, C, ...)
    - Move XY tables to correct position determined by image block and super-resolution indices.
    - Assemble image to be sent to SLM screen by selecting pixels from the plot data bitmap determined by image block and super-resolution indicated in figure 4.
    - Send image to SLM, open shutter, expose each grey level for required time based on photoresist calibration LUT.
  - Close super-resolution loop.
- Close image block loop.

2.9 Photoresist

In our experiments we use the *SHIPLEY S1800* photoresist series in layers ranging from a few hundred nm to a few microns. This resist is most sensitive at wavelengths near 436 nm but can be used between 350 and 450 nm. After exposure, the resist is developed for 2 min, using the *MICROPROSIT 303* developer diluted 1:12 with de-ionized water. This developer and dilution were chosen to give a relatively linear etch depth as a function of exposure characteristic [18]. Once suitable development parameters (dilution and development time) have been determined they are fixed and only the exposure time is varied.

3 Experimental Results

3.1 System Alignment

When setting up a stepper, several alignment steps have to be performed to obtain the specified performance: focus, parallelism of the reticle and XY table planes (out-of-plane angle), alignment of reticle axes with the XY table translation axes (in-plane angle) and XY table step distances. We first setup the photoplotter as a conventional stepper and followed the standard manufacturer's alignment procedure with a test reticle. We then adapted the standard reticle-based alignment procedure for use with our reconfigurable SLM reticle, making a series of test exposures as described below. All these alignment steps were performed without the super-resolution technique in order to better judge focus and alignment between successive image blocks. The test image used was either an all white image (all SLM pixels in the "on" state) or a specifically designed test pattern.

The first procedure is the adjustment of the auto-focus system which is adjusted manually as for a test mask reticle until the shape of the SLM pixels is as clear as possible in the centre of the optical field of view in the test plots (see figure 5). This effectively ensures that the SLM LC layer is in the object plane of the projection lens and the image plane coincides with the reference plane of the stepper system's built-in autofocus system. This alignment is set once, after which the autofocus system automatically compensates for different substrate thicknesses and planarity defects. The typical depth of field of this type of stepper is around a few microns.

The out-of-plane angle alignment is also adjusted once. It consists in placing various calibrated thickness metal shims in the SLM mount and performing test exposures until well focused SLM pixels are obtained simultaneously for all corners of the SLM.

The in-plane angle between the stages and the SLM was adjusted next. It needs to

be verified every time the prototype changes from stepper mode to photoplotter mode. However, once the SLM is aligned and fixed in its mount, this is a very quick procedure as alignment marks are included in the SLM mount which then can be aligned like any new reticle. The initial alignment is performed by exposing one all white SLM pattern, translating the stages in the X direction by a distance equal to the SLM size at the substrate level and exposing another all white pattern. This procedure is then repeated in the Y direction. When the in-plane angle is incorrectly adjusted a gap appears between the pixels of the successively exposed SLM patterns (fig. 7). When the angles (and the translation distances) are correctly adjusted the join between different etched SLM blocks is no longer visible. Figure 8 indicates an angular alignment better than 1/3 pixel (less than 1 μm) over a field of 800 pixels. More sophisticated, vernier based techniques would allow a further improvement in alignment precision but for our present applications the precision of these simple visual alignments is sufficient.

3.2 Binary Direct Write

Binary direct write consists in sending binary images to the SLM and exposing for durations such that areas of photoresist corresponding to an illuminated SLM pixel are removed completely down to the substrate when developed. Figure 9 and 10 shows the effectiveness of the photoplotter in binary direct writing. As mentioned above, the SR technique is used to fill in the "gaps" corresponding to the opaque "dead zone" between the SLM pixels. Figure 11 shows the resulting pattern in the photoresist. This, however, produces a problem, always present when the address grid is finer than the writing spot size: written structures are wider than desired. The net effect is to produce what is referred to in the binary image processing field as an image "dilatation". The solution is to precompensate the plot data (an image "erosion"), reducing the structure size by the

required amount.

The number of pixels to be eroded depends on the SLM pixel size and the SR factor. If S is the pixel size, P the pixel pitch, SR the SR factor and $A=P/SR$ the addressing grid pitch, N white pixels on the plot data should lead to a N x A etched distance in the photoresist. With the SR principle N white pixels on the image lead to a N x A + $(S - A)$ etched distance. The difference between the desired and obtained distance is therefore $S - A$ which means an erosion of $(S - A)/A$ pixels is required. As the pixel number has to be an integer, we take the nearest integer as the number of eroded pixels. Pictures of binary lines etched in photoresist without erosion and with erosion are shown in figures 12 (a) and (b). Demonstrating the effectiveness of the technique.

3.3 Multilevel Direct Write

Until recently complex 3D structures have generally been made with expensive and time-consuming multi-layer photolithographic techniques or slow, single beam direct write techniques. The use of grey-level SLMs and more especially time multiplexing techniques opens the possibility to writing multilevel structures into photoresist in a single exposure step.

In our experiments, in general 8 different levels were etched. Tests were also made successfully at 16 levels. The present limitation on the number of etched levels is imposed by the SLM refresh rate: for fixed resist thickness and development parameters the higher the number of levels the shorter the time each individual binary image present on the SLM must be exposed. At 16 levels the required image display duration was under 20 ms which is the practical limit for the nematic based LCDs used here. More levels could be produced by either using a faster SLM (see section 4.1) or by reducing the light power. The second technique would however have the drawback of reducing the overall plot rate.

In practice, in many cases 8 levels are usually sufficient since when used with large SR factors, the write pixels overlap because the width of the writing pixel covers several address grid points and hence an overlap of light from neighbouring points occurs. This produces a smoothing effect which leads to practically continuous relief profiles such as those shown in figure 13.

A wide range of 3D structures including cones, pyramids and circular, elliptic, spherical or aspherical microlenses have been realised with the multilevel direct writing technique. Figure 14 shows an example of the sort of structures that can be written by multilevel direct write. Figure 15 demonstrates the level of control that has already been achieved: a vertical resolution of better than 50 nm into 1 micron photoresist layers. Through use of suitably designed calibration tables we were also able to direct write binary and multilevel structures side by side on the same substrate in the same exposure step.

3.4 Resolution

The minimum feature size of plotted structures is determined by the lens reduction factor and the SLM pixel size. With our SLM and the 5× reduction lens, the minimal feature size written in the photoresist is the photoreduced pixel size $5\times3\ \mu\mathrm{m}^2$ corresponding to the transparent central part of the SLM pixel. However through the use of the high resolution XY tables and the SR technique it is possible to apply a much smaller address grid as the XY tables can make steps down to 40 nm. We typically use a 1.1 micron address grid. By suitable preparation of the plot data files and allowance for the "dilatation" effect mentioned above, it is possible to produce "unetched" binary structures down to the optical resolution of the system, here about 1 μm - see fig. 16. As an illustration, an uncompensated data file with a 1 micron address grid containing 1 pixel vertical lines separated by 5 pixel gaps would produce 5 micron lines separated by 1 micron gaps due

to the 5 micron width of the SLM pixels. Hence with our present system in a positive resist we can build 1 μm structures with 3 or 5 μm gaps. In a negative resist we can build 3 to 5 μm structures with 1 μm gaps.

3.5 Plot Rate

On the present prototype a binary pattern of 600x800 pixels (entire SLM) giving a 6.6 μm photoresist level pixel pitch is plotted with an exposure of less than 200 ms which gives a basic 2.4 Mpixels/s or 2.9 mm^2/s plot rate. For multilevel structures exposure time and hence plot rate depend on the local structure etch depths - typically exposure steps of about 20 ms per layer are required giving overall plot rates that are relatively similar to the binary case. Super-resolution translation distances are very short so do not greatly reduce the overall plot rate. The translations between the different image blocks, however, are greater and do reduce overall plot rate. Exact rates obtained depend on plot data but typical average values are of the order of a cm^2/min.

4 Discussion

The current performance of the photoplotter described above is already competitive in terms of plot rate and resolution in a number of the application fields mentioned in the introduction, particularly in terms of cost and flexibility. However, the performance can also be improved relatively simply. We now discuss the current and more fundamental limitations on photoplotters based on SLM reticles for photolithographic steppers and ways of overcoming these limitations.

4.1 Plot rate

The plot rate can be improved in 3 major ways. The first and simplest is to use more recent LCDs with higher pixel counts: compatible 1024x768 and 1280x1024 pixels LCDs are now commercially available and even higher, HDTV driven, pixel counts now appearing or planned. The maximum refresh rates of these new microdisplays are at least as high as our current SLM so factor three to four increases in plot rate are immediately available for very minor modification to the system. In addition, as LCD microdisplay technology progresses in the future, plot speed will be increased accordingly, the only change being required in the photoplotter is a modified LCD mount and when necessary a more recent video card.

The second way to improve plot rate also concerns the SLM. The current plot rate is limited by the maximum display rate on the LCD. By using recent, alternative, commercially available microdisplay technologies such a Liquid Crystal on Silicon (LCOS) [19], Ferroelectric Liquid Crystal (FLC) [20, 21] and Texas Instrument's Digital Micromirror device (DMD) light modulator, technologies significantly higher refresh rates could be achieved. LCOS is a reflective technology where liquid crystals are present over the surface of a silicon chip coated with a reflective aluminized layer. The opaque inter-pixel space is greatly reduced because the control circuit is in the silicon backplane, thus increasing optical efficiency. The close link between drive electronics and each pixel also greatly simplifies image update often resulting in significantly improved display refresh rates. FLC devices use liquid crystal substances that have chiral molecules in a smectic C arrangement and allow microsecond switching times - often more than an order of magnitude faster than nematic LC based devices. DMD technology consists of hundreds of thousands of moving micromirrors which are controlled by underlying CMOS electronics [12, 13]. Such devices can reach frame rates of 9800 Hz.

The practical use of such technologies is, however, not as straightforward as using higher pixel count transmissive LCDs. These new technologies are reflective so a major redesign of the display illumination system would be required. Another practical difficulty concerns getting the plot data onto the devices quickly enough to be able to access such high refresh rates. Standard video cards are designed for the human eye so generally have maximum refresh rates in the 100 Hz range. Custom designed drive electronics are now appearing for some devices but they are very significantly more expensive. Currently the best compromise appears to be to use mass market PC video cards and drivers which allow maximum refresh rates in the 100 Hz range. By using the three colour channels (RGB) to each display monochrome plot data, the effective refresh rate can be tripled.

The other practical difficulty is that if such refresh rates can be achieved, plot rate will then be limited by available light power. The reflective technologies help in this direction as they generally have higher fill factors and hence optical efficiency. However, with our current system, refresh rates in excess of 100 Hz (corresponding to a 10 ms display time for a given etch depth level in a multilevel plot) would again require an illumination system redesign with a higher power light source and perhaps a different light source such as a pulsed laser, adding considerable complexity and expense.

The third, linked, technique for increasing plot rate is to use "on-the-fly" plotting in which the XY tables move continuously. This would remove the need to wait for the tables to reach the desired position and stabilise before exposing each SLM image. In this way the full refresh rate of the SLM could be used at all times, significantly increasing the overall plot rate. The application of "on-the-fly" plotting, however, would entail a major modification of the current system since a high power, short duration, pulsed source would be required along with redesigned XY table drive electronics and software to be sure of a clearly exposed image. Problems such as potential SLM damage due to the high optical

pulse power would also have to be addressed. These factors would make the reuse of existing steppers much more complicated: a complete system redesign would be required, greatly increasing costs and losing the advantages of the approach proposed here.

4.2 Resolution

As indicated above, the smallest feature size of plotted structures (3x5 micron structures with 1 micron gaps) is limited by the lens reduction factor and the SLM pixel size. The resolution can be improved simply in two ways: using an SLM with smaller pixels and using a lens with a greater reduction factor.

As SLM pixel count has increased in recent devices, the pixel size has tended to decrease so simply replacing the existing SLM with a more recent one would improve both the plot rate and resolution. Typical current transmissive LCD microdisplays of the type mentioned in section 4.1 have pixel pitches of 15-20 μm with active areas of around 10-15 micron giving a roughly factor two gain in minimum feature size. Reflective LCOS or DMD generally have significantly smaller pixels (less than 10 μm for the most recent LCOS devices, giving improved resolution at the expense of a redesigned illumination system).

Changing lens reduction factor is also a relatively simple way to increase resolution as 10:1 and 20:1 reduction factor lenses already exist for the type of stepper used as the basis for our photoplotter. Thus by combining smaller SLM pixels and available reduction factor lenses it is relatively simple to reach resolutions limited by the resolving capabilities of the reduction lens - roughly 1 μm for the g-line steppers compatible with LCD SLMs.

Going to features sizes smaller than this would require the use of lenses optimised for shorter UV wavelengths (for example i-line). This, however, is problematic with standard LCD devices since LC molecules can be damaged by UV light and good quality

compatible polarisers are more difficult to find at these wavelengths. To be able to use such wavelengths other SLM technologies such as DMD are required, which in turn means the stepper illumination system would have to be redesigned to take account of the reflective display - again losing many of the advantages of the approach proposed here.

5 Conclusion

In this paper we have shown that, by combining a standard transmissive liquid crystal microdisplay with an existing g-line photolithographic stepper, a highly versatile direct-write photoplotter can be built simply and relatively cheaply. The resulting system has a respectable performance as a photoplotter in terms of resolution, plot rate and cost. In addition, thanks to the drop-in nature of the microdisplay module, the photoplotter can be simply converted to a standard stepper in a few minutes. As such it is particularly adapted for R&D labs and custom or short production runs. The same equipment can be used for both binary plots (*e.g.* for chrome photomask fabrication) and for the production of 3D microstructures by grey-level, direct write into photoresist. The only change between these two operating modes is the control software, indeed the simultaneous plotting of binary and multilevel data on the same substrate has also been demonstrated. The present performance can be very easily improved in both resolution and plot rate thanks to ongoing improvements in LCD technology. We have discussed the current limitations on the approach and proposed ways of overcoming them.

Our current work in the field is centred on improving the resolution performance in two separate ways. The first involves a new prototype based on the same principle and software but with a stronger reduction factor lens and a reflective micromirror device in place of the LCD microdisplay to enable a lower wavelength UV source to be used.

The second resolution enhancing technique under investigation concerns the application

of proximity correction techniques on the plot data. The surface relief obtained with the photoplotter can be modelled as the convolution of the point-spread function (PSF) of optical instrument with the desired relief profile which would have been obtained in the absence of this smoothing effect [18, 22, 23]. This technique is well known in single beam direct write applications and several techniques exist for precompensating the plot data to correct for this smoothing and hence obtain plots closer to the desired profile [18, 22–27]. Adaptation of these techniques to our massively parallel photoplotting technique with our non-standard write beam profiles and individually variable power levels is already showing promising results and will be presented in a future paper.

Acknowledgements

This research was mainly funded by EC through the CRAFT DRAWMAP project. We also acknowledge the contribution of PM Professional Maintenance in setting the stepper and Carole Moussu and Andreas Weber in the initial stages of this work.

References

[1] M. B. Stern, "Binary optics fabrication," Chap. 3 in *Micro-optics: elements, systems and applications*, H. P. Herzig, pp. 53–86, CRC Press, Cornwall (1997).

[2] N. Dumbravescu, "Experiments for 3-D structuring of thick resists by gray tone lithography," *Materials Science in Semiconductor Processing*, 3, 569–573 (2000).

[3] H. Yu, B. Li, and X. Zhang, "Flexible fabrication of three-dimensional multi-layered microstructures using a scanning laser system," *Sensors and Actuators A*, 125, 553–564 (2006).

[4] N. Matsuzuka, Y. Hirai, and O. Tabata, "A novel fabrication process of 3D microstructures by double exposure in deep x-ray lithography (D^2XRL)," *J. Micromech. Microeng.*, 15, 2056–2062 (2005).

[5] N. Yamazaki, T. Yamaguchi and H. Namatsu, "Three-dimensional nanofabrication with 10-nm resolution," *Jpn. J. Appl. Phys.*, 43(8B), 1111–1113 (2004).

[6] T. Osipowicz, J. A. van Kan, T. C. Sum, J. L. Sanchez, and F. Watt, "The use of photon microbeam for the production of microcomponents," *Nucl. and Meth. B*, 161-163, 83–83 (2000).

[7] H. Martinsson, T. Sandstrom, A. Bleeker, and J. D. Hintersteiner, "Current status of optical maskless lithography," *J. Microlith., Microfab., Microsyst.*, 4(1), 011003 (2005).

[8] R. Menon, A. Patel, D. Gil, and H. I. Smith, "Maskless lithography," *Materials Today*, 8, 26–33 (2005).

[9] M. T. Gale, M. Rossi, H. Schütz, P. Ehbets, H. P. Herzig and D. Prongué, "Continuous-relief diffractive optical elements for two-dimensional array generation," *Appl. Opt.*, 32(14), 2526–2533 (1993).

[10] F. Nikolajeff, S. Jacobsson, S. Hård, Å. Billman, L. Lundbladh and C. Lindell, "Replication of continuous-relief diffractive optical elements by conventional compact disc injection-molding techniques," *Appl. Opt.*, 36(20), 4655–4659 (1997).

[11] Q. Peng, S. Liu, Y. Guo, B. Chen, J. Du, and Y. Zeng, "Real-time photolithography technique for fabrication of arbitrarily shaped microstructures," *Opt. Eng.*, 42(2), 477–481 (2003).

[12] Y. Gao, T. Sheng, J. Chen, N. Luo, X. Qi, and Q. Jin, "Research on high-quality projecting reduction lithography system based on digital mask technique," *Optik*, 116, 303–310 (2005).

[13] L. Chi, G. Xiaowei, G. Fuhua, L. Boliang, D. Xi, D. Jinglei, and Q. Chuankai, "Imaging Simulation of Maskless Lithography Using a DMD™," *Proc. SPIE*, 5645, 307–314 (2005).

[14] TL Electronic GmbH, http://www.tl-electronic.de/

[15] H&L Associates, http://www.trilicium.ca/hl_index.php/

[16] KRFTech ltd. changes names to Jungo ltd., http://www.jungo.com/

[17] MIVA Technologies GmbH, http://www.mivatec.com/

[18] P. Ehbets, M. Rossi, and H. P. Herzig, "Continuous-relief fan-out elements with optimized fabrication tolerances," *Opt. Eng.*, 34(12), 3456–3463 (1995).

[19] K. M.Johnson, D. J. McKnight, and I. Underwood, "Smart spatial light modulators using liquid crystals on silicon," *IEEE Journal of Quant. Electr.*, 29(2), 699–714 (1993).

[20] Displaytech Inc., http://www.displaytech.com/

[21] Forth Dimension Displays Ltd., http://www.crlopto.com/

[22] J. Bengtsson, "Direct inclusion of the proximity effect in the calculation of kinoforms," *Appl. Opt.*, 33(22), 4993–4996 (1994).

[23] M. Ekberg, F. Nikolajeff, M. Larsson, and S. Hård, "Proximity-compensated blazed transmission grating manufacture with direct-writing, electron-beam lithography," *Appl. Opt.*, 33(1), 103–107 (1994).

[24] L. Grella, E. Di Fabrizio, M. Gentili, M. Baciocchi, and R. Maggiora, "Proximity correction for e-beam patterned sub-500nm diffractive optical elements," *Microelectron. Eng.*, 35, 495–498 (1997).

[25] H. Zhang, J. Morrow, and F.M. Schellenberg, "Optical proximity correction: a detail comparison of techniques and their effectiveness," *Microelectron. Eng.*, 41/42, 79–82 (1998).

[26] J. Du, Q. Huang, J. Su, Y. Guo, and Z. Cui, "New approaches to optical proximity correction in photolithography," *Microelectron. Eng.*, 46, 73–76 (1999).

[27] L. Veneklasen, U. Hofmann, L. Johnson, V. Boegli, and R. Innes, "Run-time correction of proximity effects in raster scan pattern generator systems," *Microelectron. Eng.*, 46, 191–195 (1999).

Biographies

Mélanie Kessels received her University degree and her M.Sc. in Physics Sciences from the University of Liège (BELGIQUE) in 2003 and 2005, respectively. She is presently working towards the Ph.D. degree in Engineering Sciences at the Ecole Nationale Supérieure des Télécommunications de Bretagne (E.N.S.T.) in Brest (FRANCE).

Dr. Kevin Heggarty received his B.A. in Natural Sciences from the University of Cambridge (UK) in 1987, his M.Sc. in Telecommunications and Information Systems from the University of Essex (UK) in 1988 and his doctorate from the Ecole Nationale Supérieure des Télécommunications (E.N.S.T.) in Paris (FRANCE) in 1991. He is now senior lecturer at the ENST Bretagne. His research interests include non-display applications of spatial light modulators, the design and fabrication of diffractive micro-optical elements and their applications in optical telecommunications and optical information processing

in general.

List of Figures

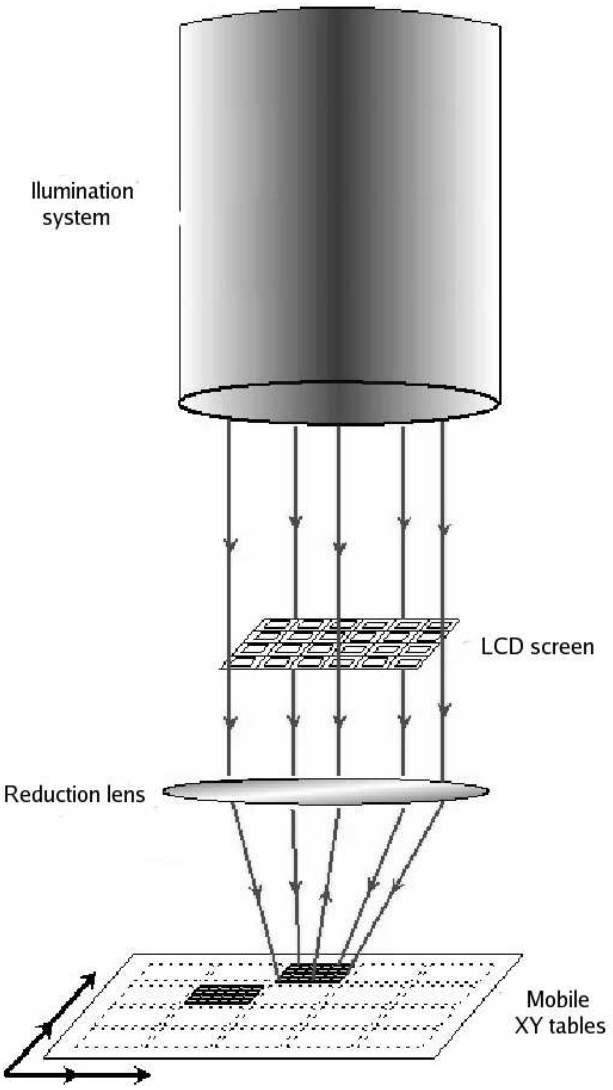

Figure 1: Parallel write photoplotter basic principle. Illumination system illuminates the LCD. The LCD is imaged onto photoresist coated substrate with a reduction factor lens.

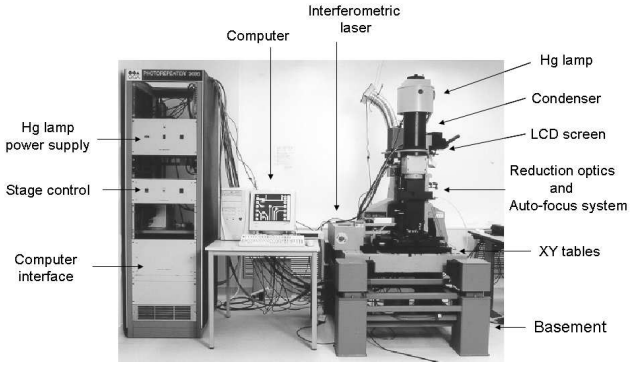

Figure 2: GCA 4800DSW photorepeater converted into a photoplotter.

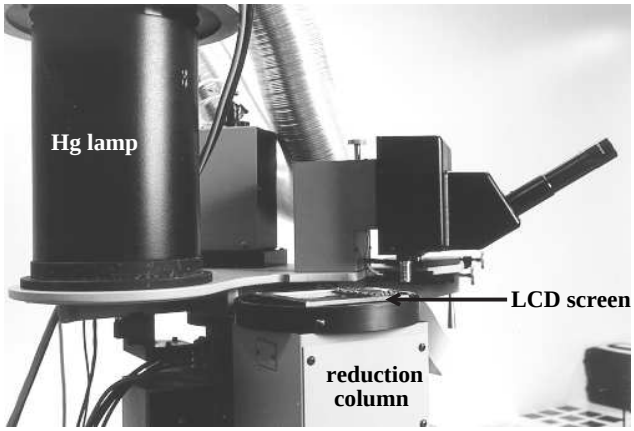

Figure 3: Microdisplay mounted on the photorepeater. The SLM module is positioned using a specially adapted mount on the top of the reduction column such that the LC plane is in the same optical plane as a standard photolithographic reticle.

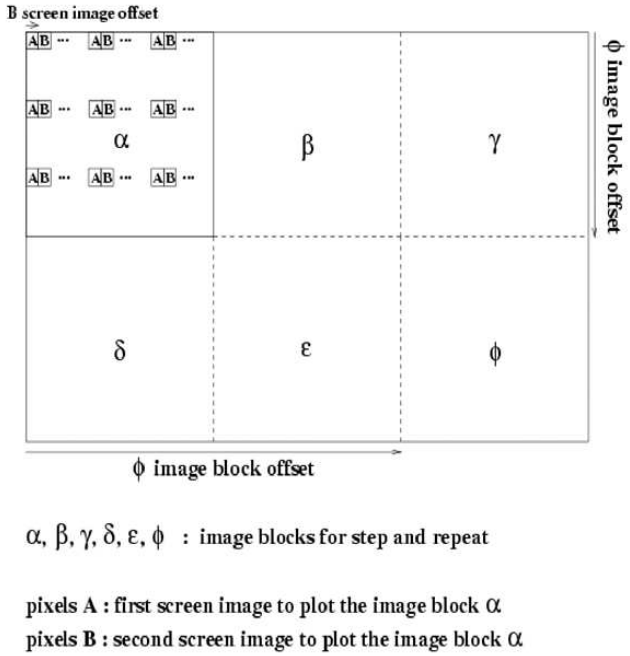

Figure 4: "Block plotting" and "super-resolution" principle. The plot data is cut into 6 blocks ($\alpha, \beta, \gamma, \delta, \varepsilon$ and ϕ) whose size equals the SLM size. The first block α is plotted using the "super-resolution" technique. At the moment of the first illumination, the pixels A are displayed on the SLM, then the pixels B, then C, ... until the whole block α is plotted. The same steps are used to plot block β, then block δ, ...

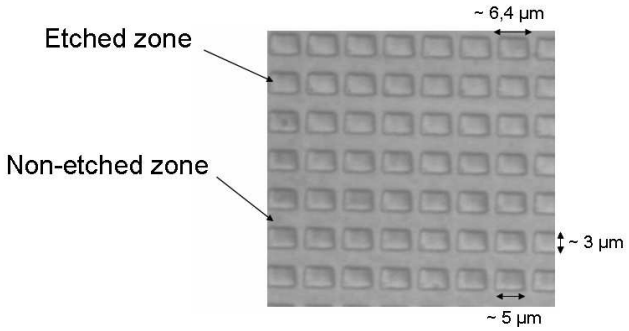

Figure 5: Photograph of a part of the pixel array etched into photoresist corresponding to an LCD screen where all pixels are in the ON state (transparent).

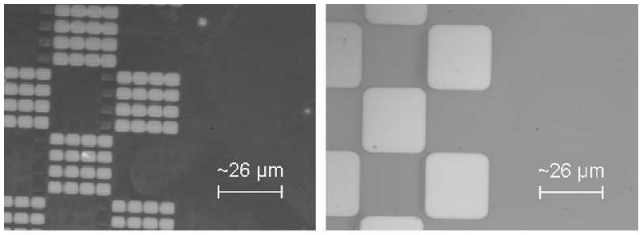

Figure 6: Comparison between etched patterns (a) without and (b) with the SR technique. In (a) LCD screen pixels are visible. In (b) the SR technique eliminates the pixelisation effect.

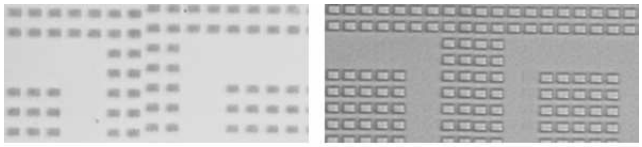

Figure 7: The relative angle between the XY stages and the screen must be adjusted. (a) Bad relative angle adjustment: pixels on the block boundaries are badly aligned. (b) Relative angle is adjusted: block boundary etched screen pixels are aligned.

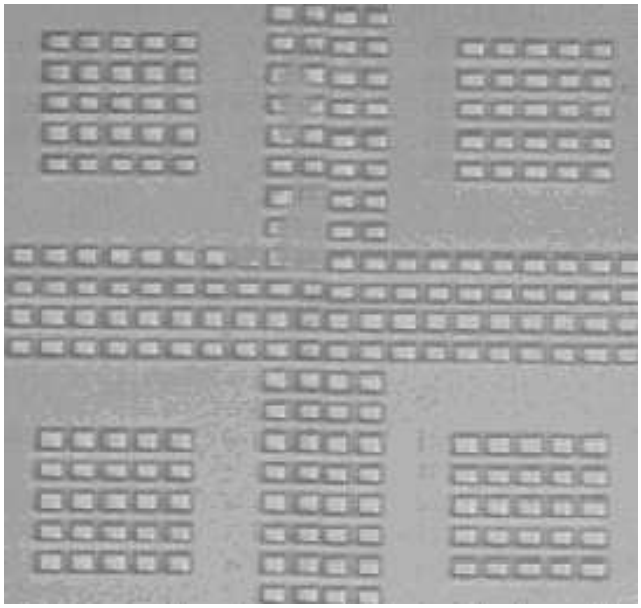

Figure 8: A test file is used to verify screen alignment: auto-focus, angular alignment and junction between etched screens.

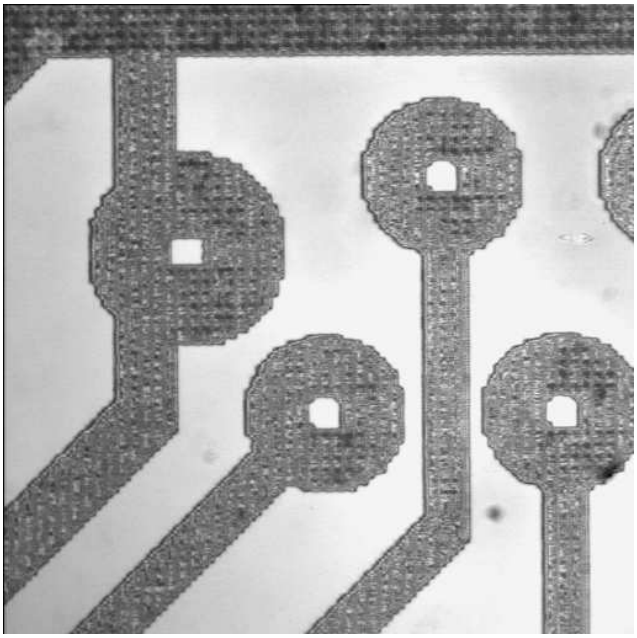

Figure 9: View of a binary direct-write plot in photoresist from a PostScript file.

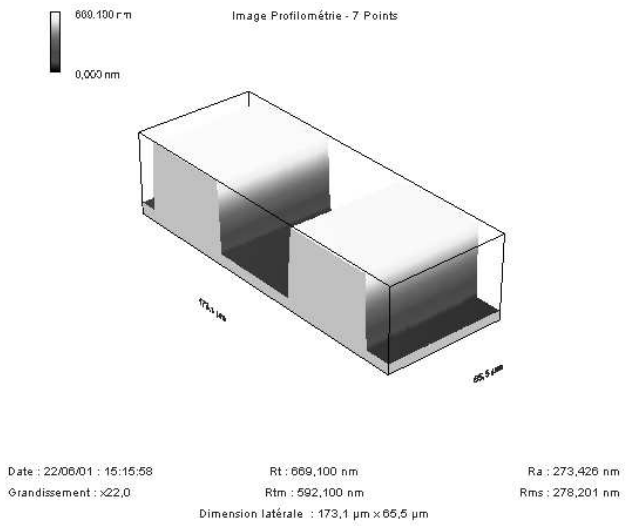

Figure 10: A 3D view of a directly written grating in photoresist obtained using an interferometric microscope. A flat surface in the upper unexposed areas and in the lowest level areas (indicating complete removal of the photoresist) and steep edges between the 2 flat surfaces are visible.

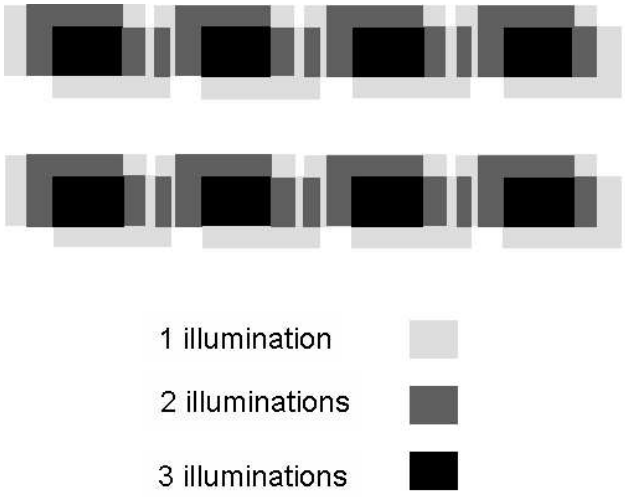

Figure 11: When plotting binary images with the SR technique, successive exposures etch the desired image in the photoresist. Between the successive exposures, the substrate moves. Each photoresist area is exposed differently as a function of the number of received exposures. In this example, the photoresist has been exposed to 3 SLM patterns. The pixel overlap areas have been exposed three times. The different grey levels code different etch depths. The darker the area, the more illuminated and then the more exposed in the photoresist.

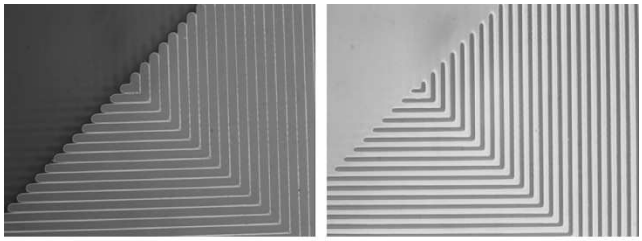

Figure 12: Pictures of binary lines etched in photoresist (a) without erosion and (b) with erosion shown. Etched and non-etched lines should be of 5 μm width. (a) When the image to be plotted is not precompensated, the etched lines are larger than the non-etched lines. (b) When lines are correctly precompensated on the image to be plotted, etched and non-etched lines are of equal width as desired.

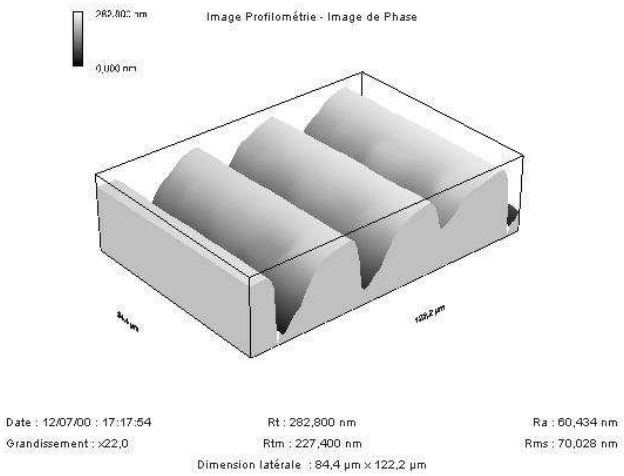

Figure 13: A 3D view of continuous relief diffractive structure obtained by direct write. The smooth surface is obtained thanks to a high SR factor.

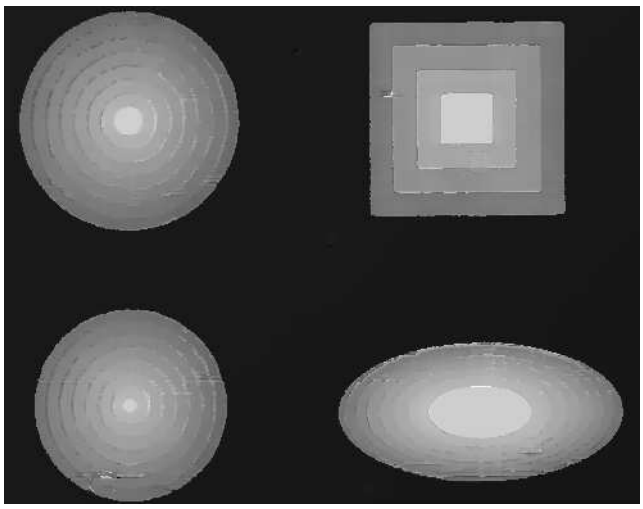

Figure 14: A 2D interferometric microscope plot of different shapes simultaneously directly written into photoresist. The different grey levels code different etch depths.

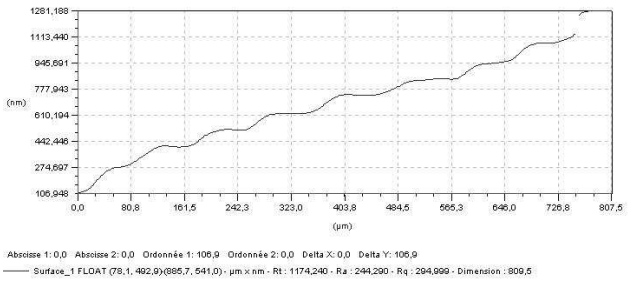

Figure 15: A 2D slice through a multilevel staircase diffraction grating obtained by direct write into photoresist showing a depth control precision better than 50 nm.

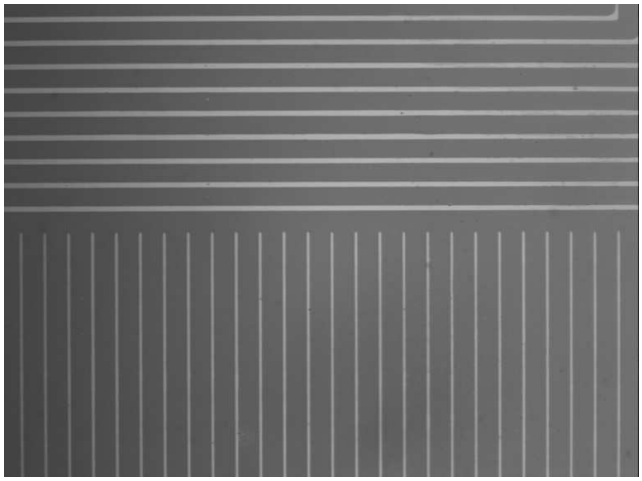

Figure 16: By using the SR technique it is possible to use a much smaller address grid (here 1.06 μm) and hence leave gaps between "written" structures of down to 1 μm. On this figure, horizontal etched 8 μm width lines with 2 μm unetched gaps and, vertical etched 9 μm width lines with 1 μm unetched gaps are plotted.

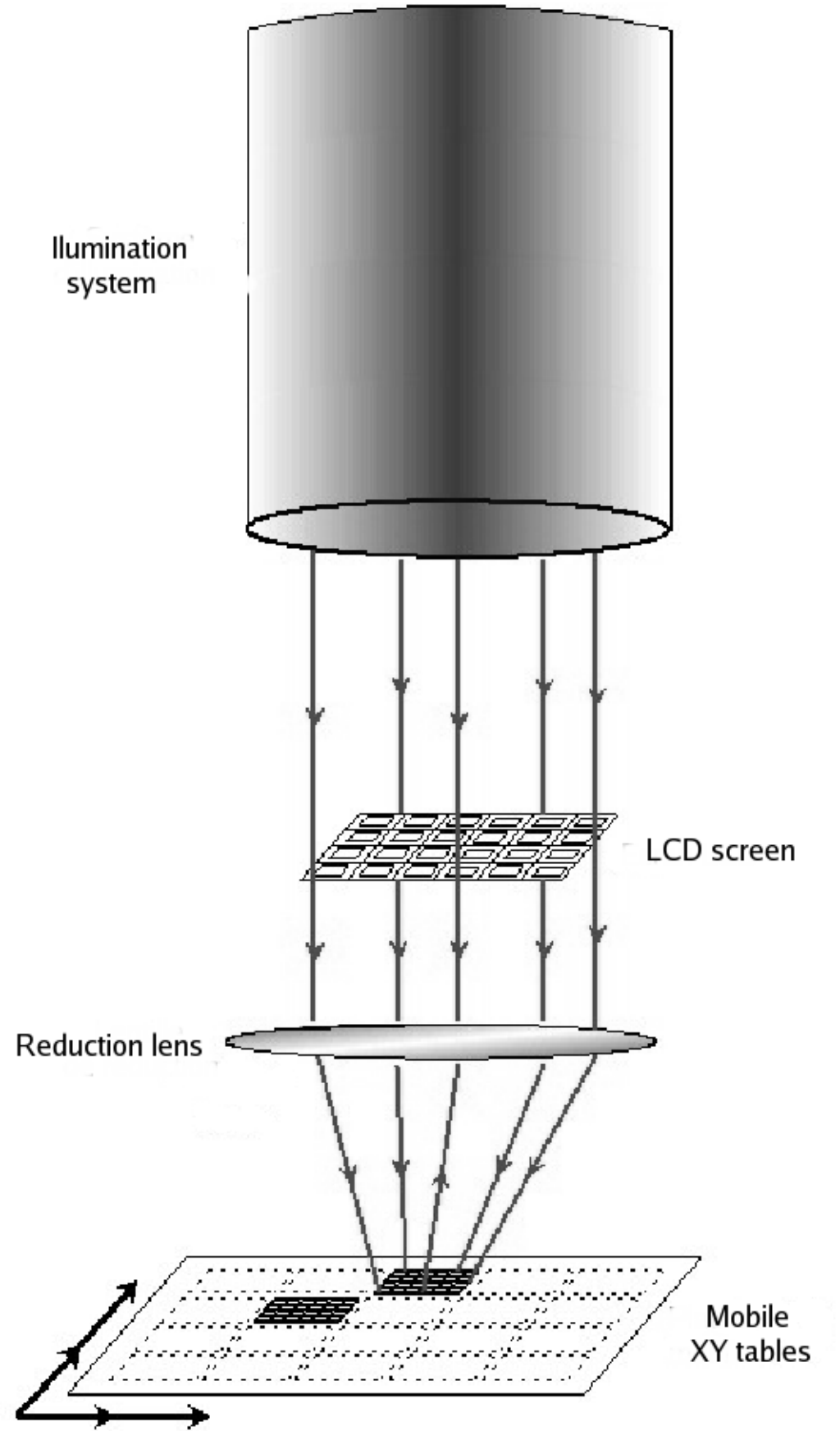
Illumination system
LCD screen
Reduction lens
Mobile XY tables

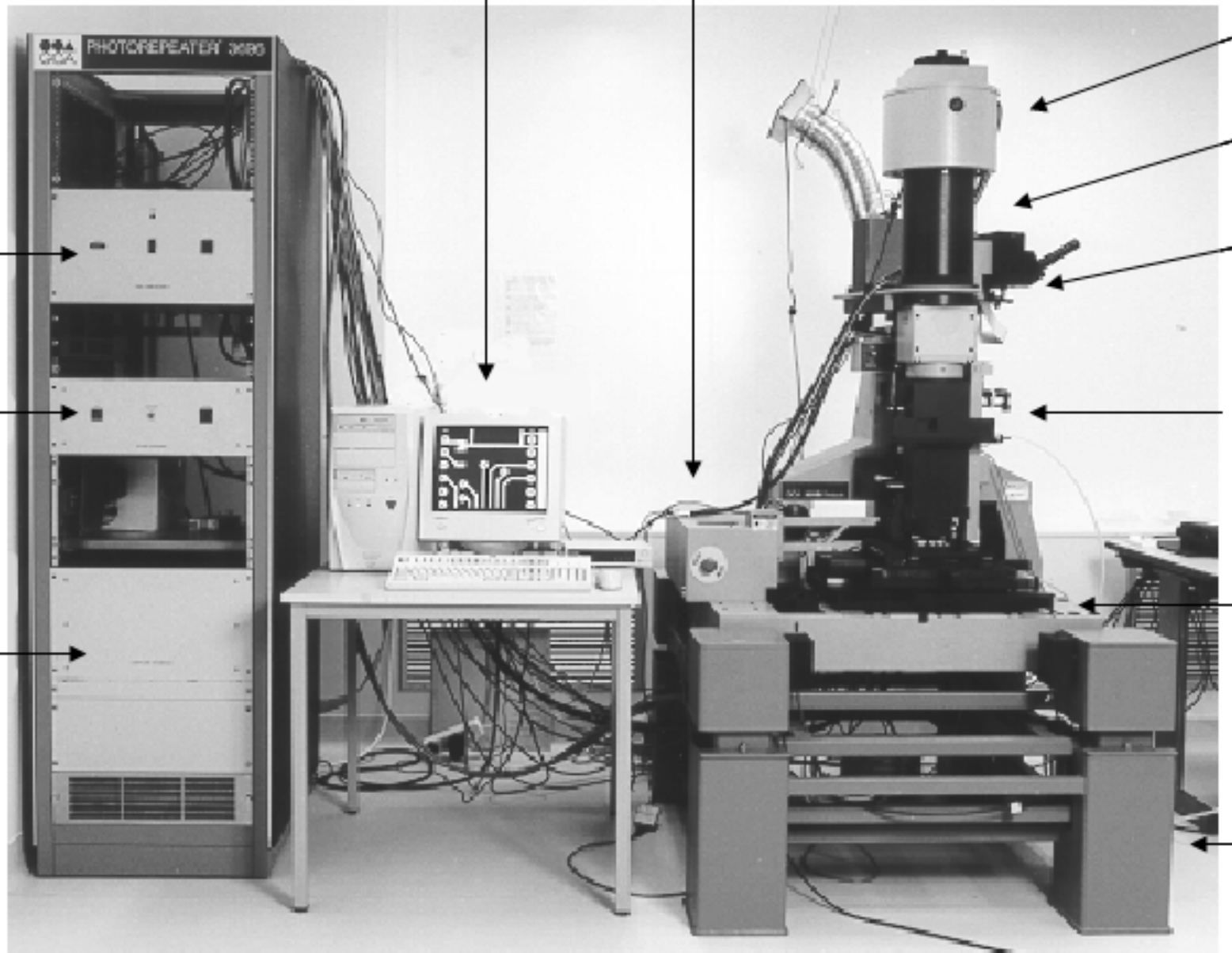
Interferometric laser
Computer
Hg lamp
Condenser
LCD screen
Hg lamp power supply
Reduction optics and Auto-focus system
Stage control
XY tables
Computer interface
Basement

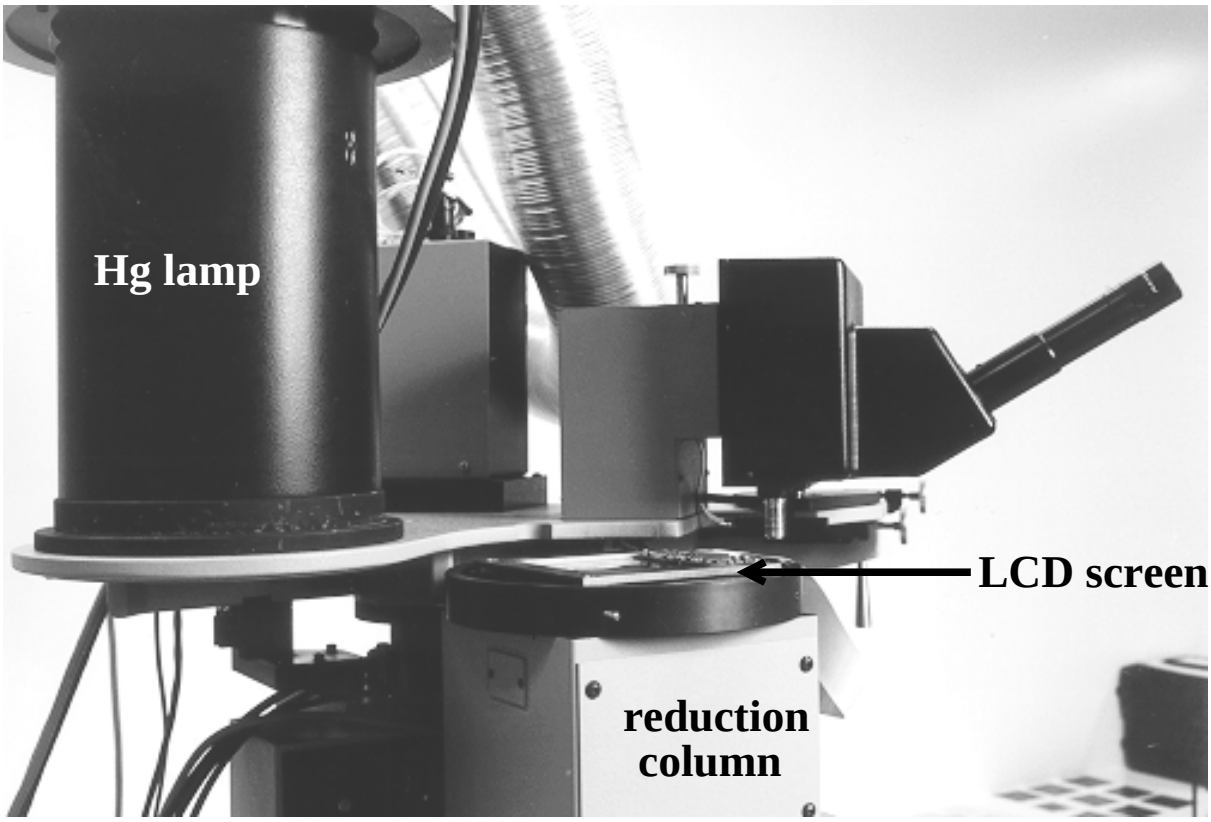
Hg lamp
LCD screen
reduction
column

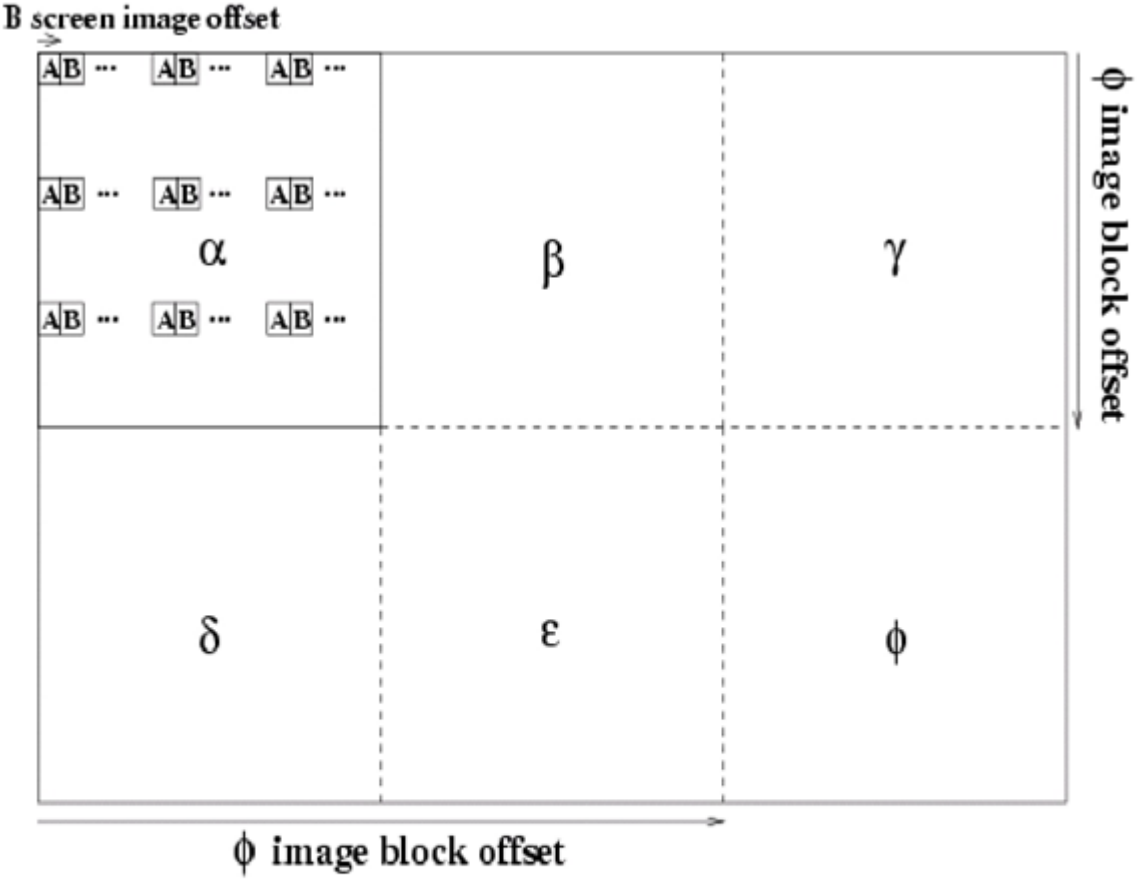

α, β, γ, δ, ε, ϕ : image blocks for step and repeat

pixels **A** : first screen image to plot the image block α

pixels **B** : second screen image to plot the image block α

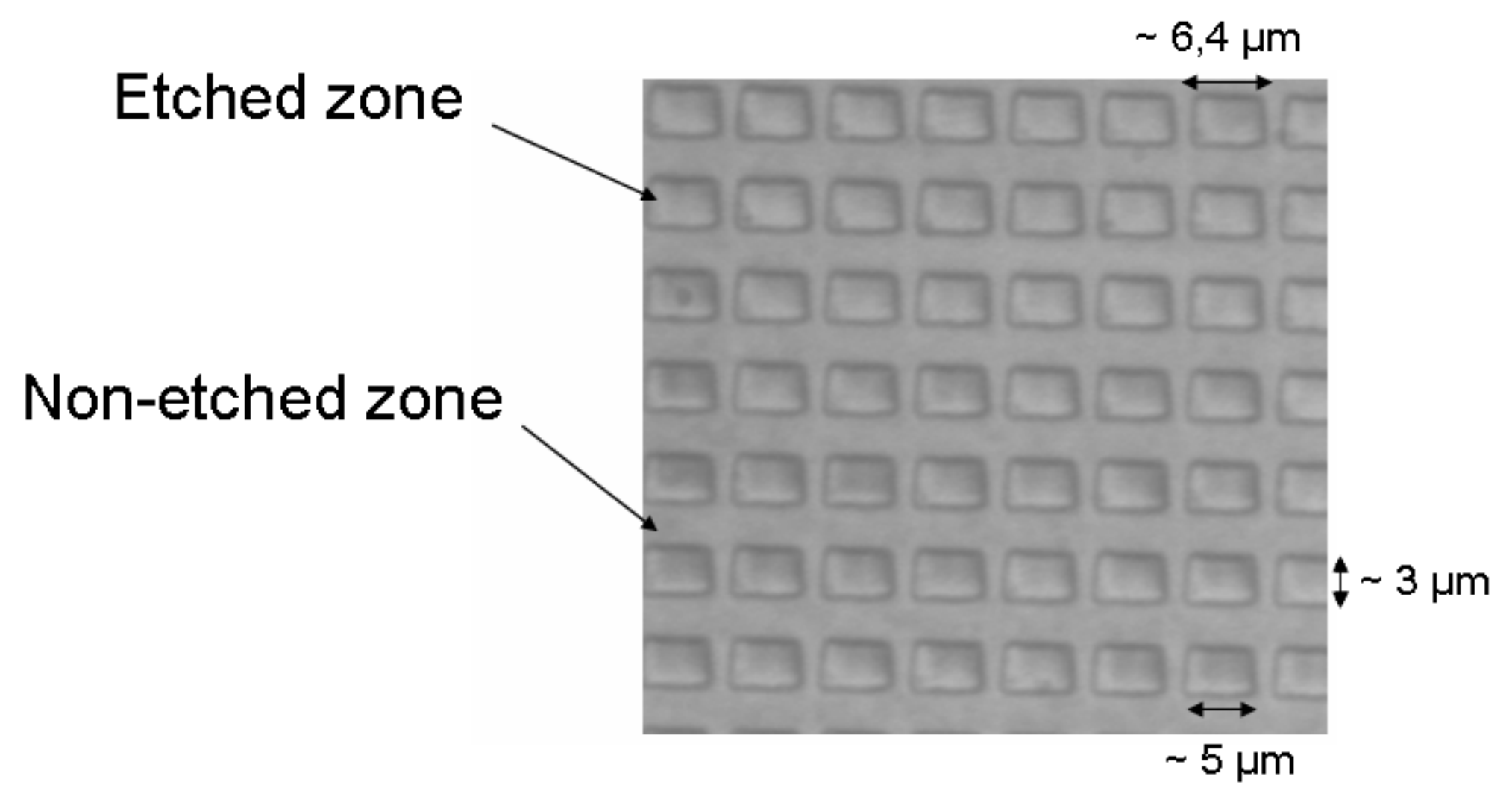
~ 6,4 µm
Etched zone
Non-etched zone
~ 3 µm
~ 5 µm

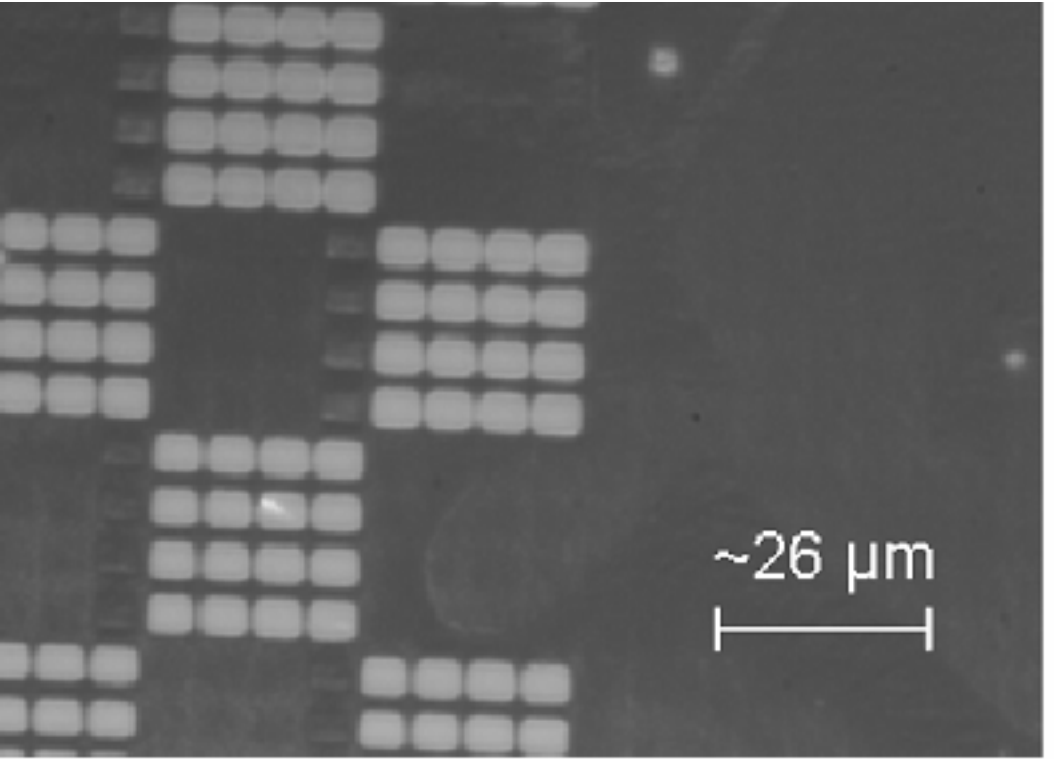

(a) Without SR technique

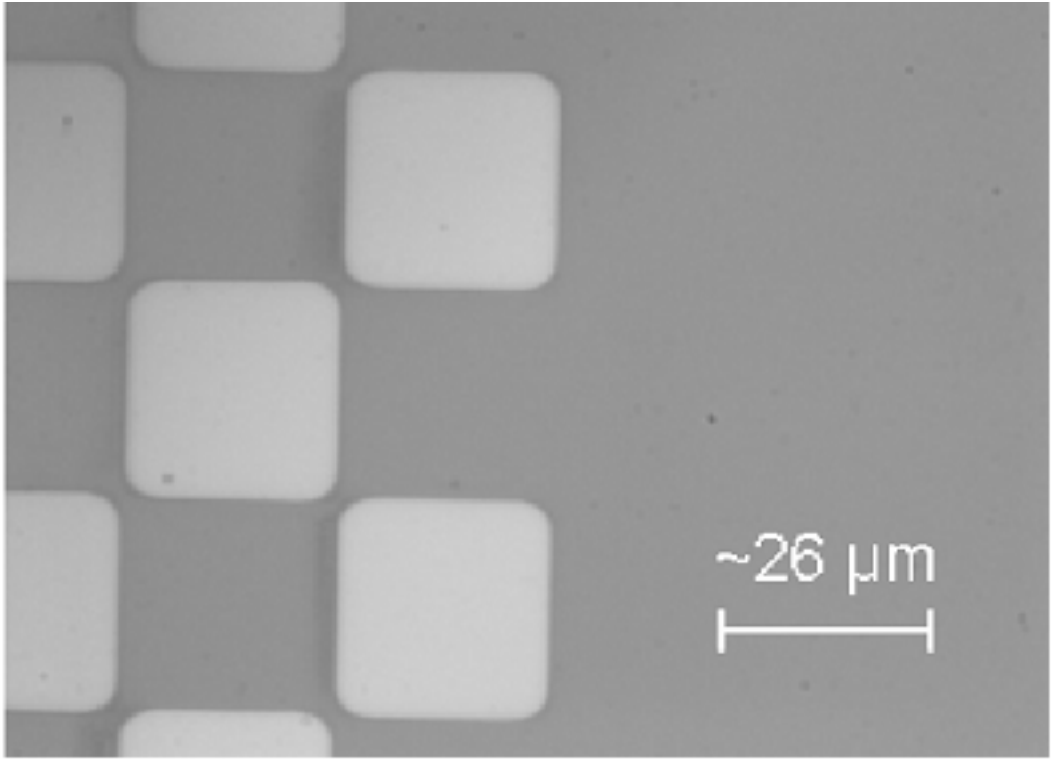

(b) With SR technique

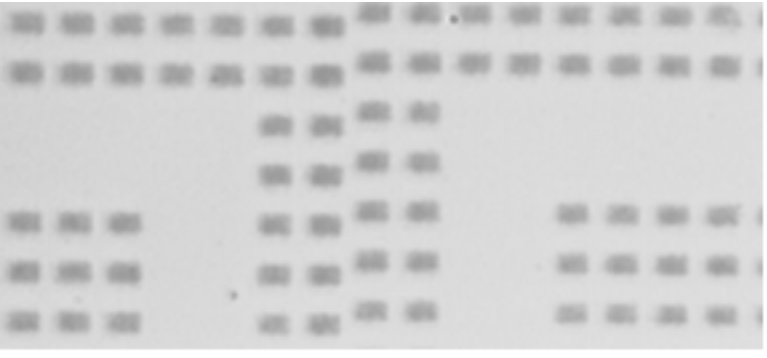

(a)

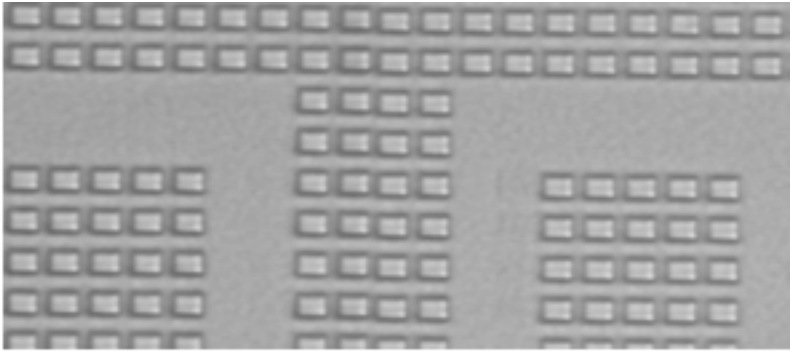

(b)

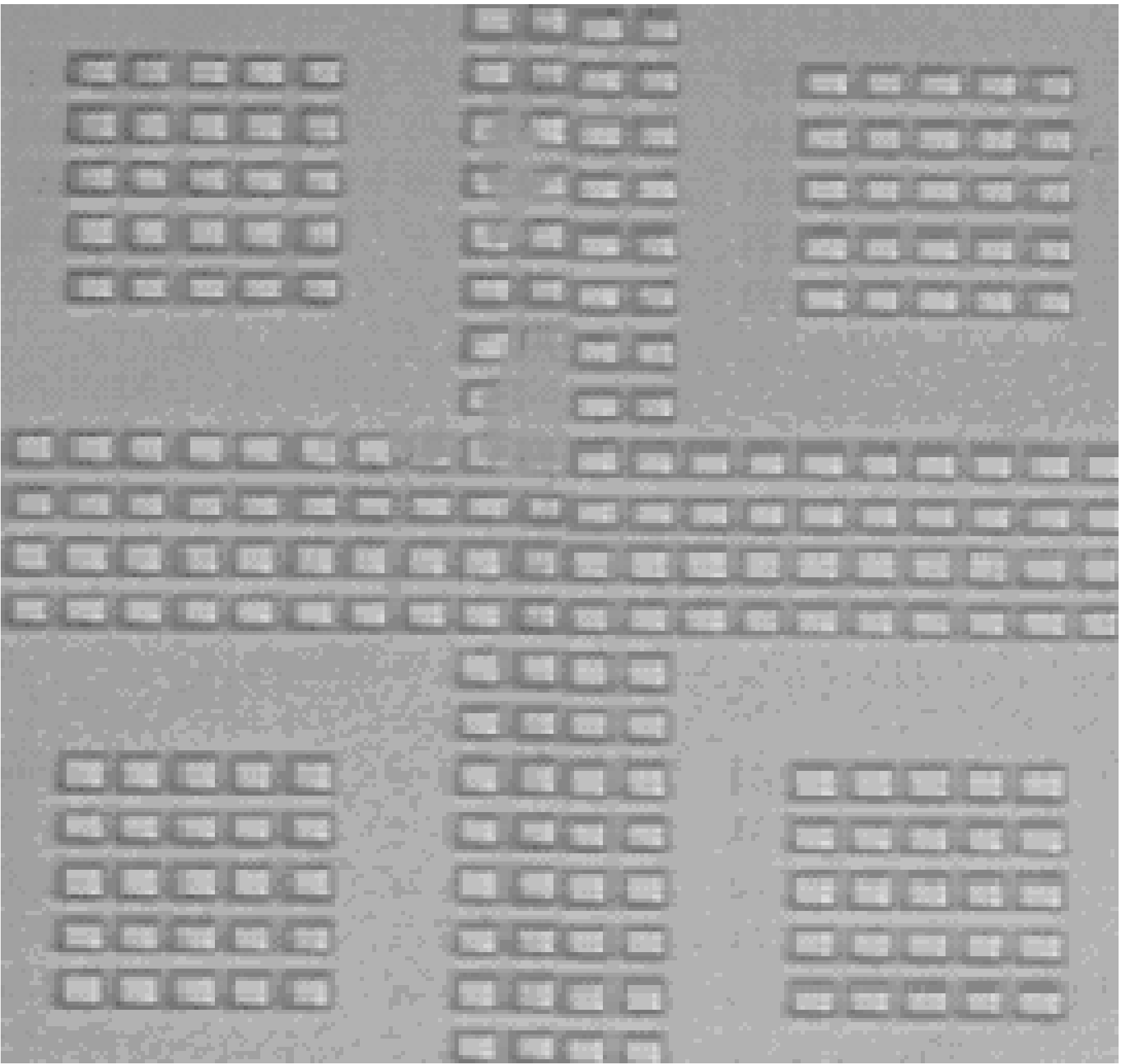

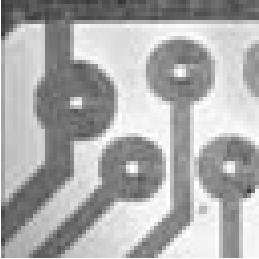

669,100 nm

0,000 nm

Image Profilométrie - 7 Points

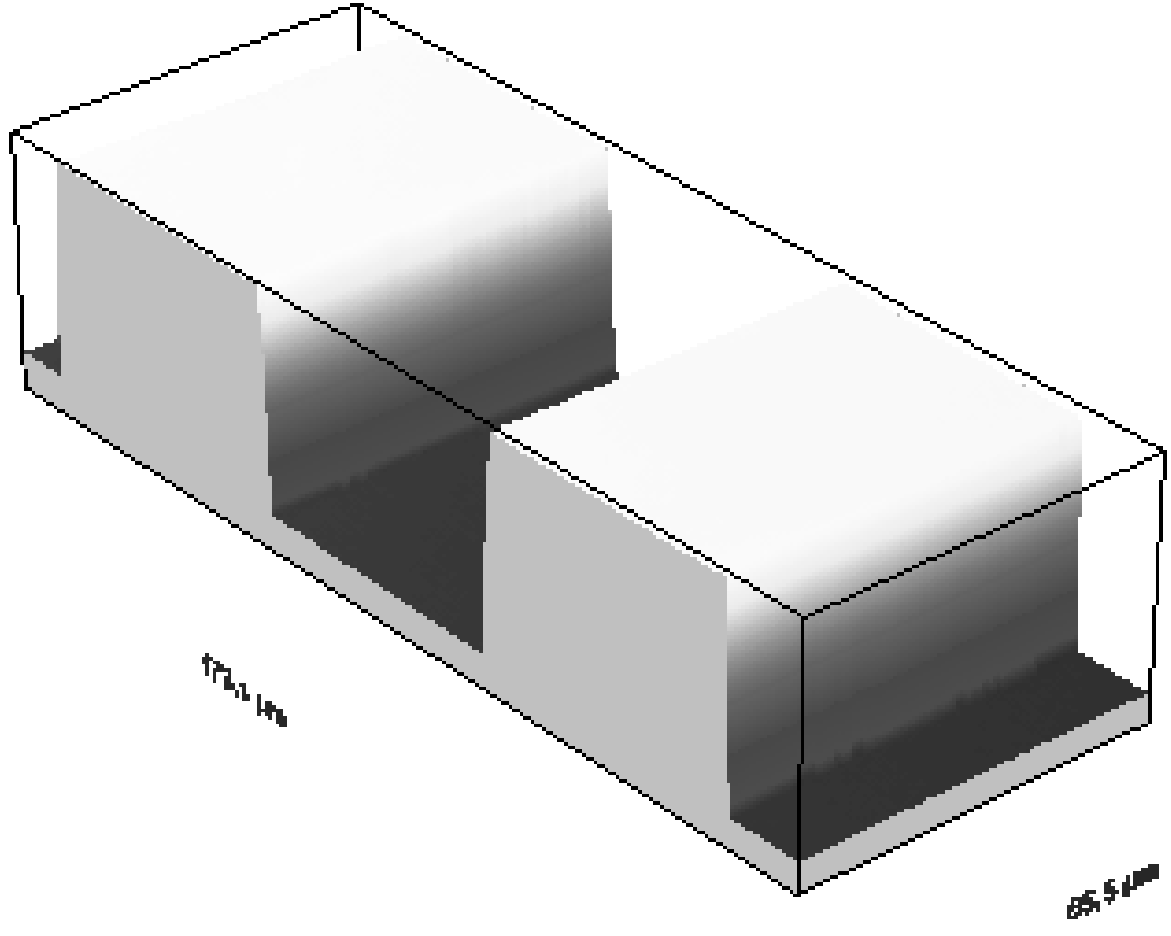

Date : 22/06/01 : 15:15:58

Rt : 669,100 nm

Ra : 273,426 nm

Grandissement : x22,0

Rtm : 592,100 nm

Rms : 278,201 nm

Dimension latérale : 173,1 µm x 65,5 µm

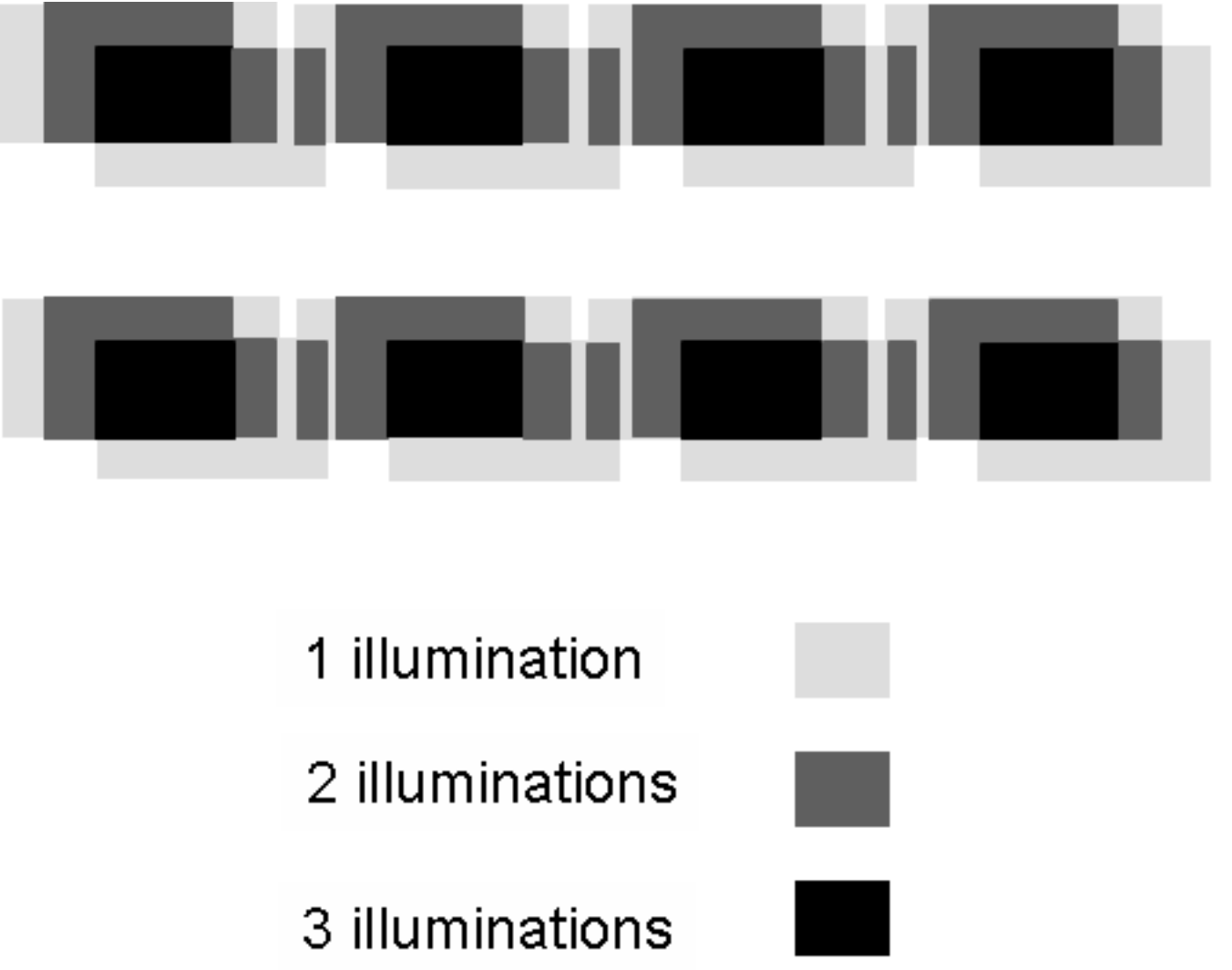
1 illumination
2 illuminations
3 illuminations

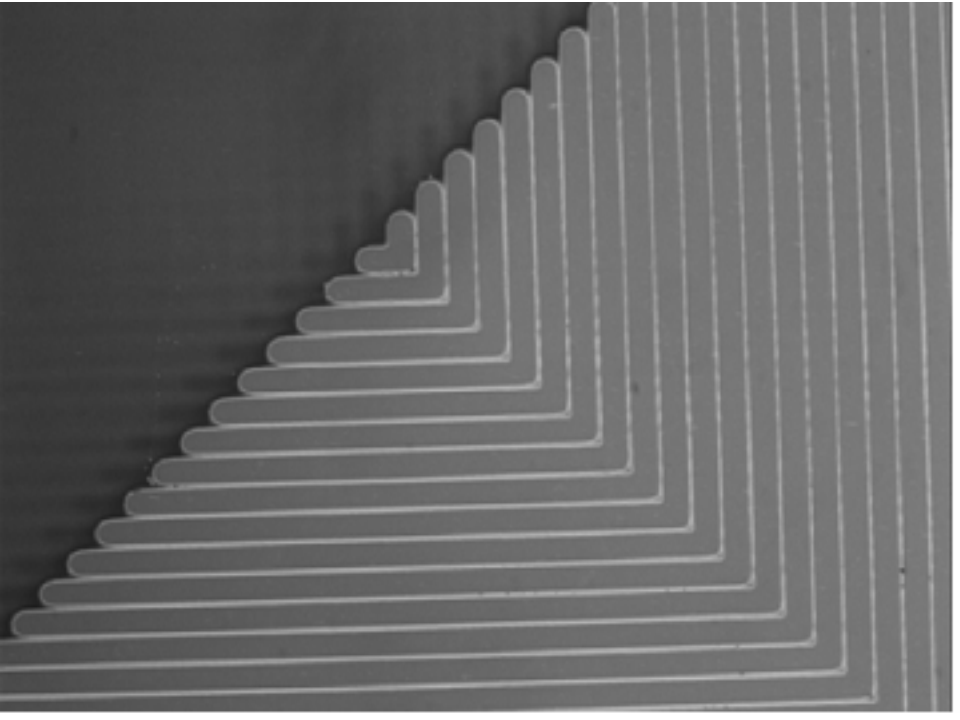

(a) Without erosion

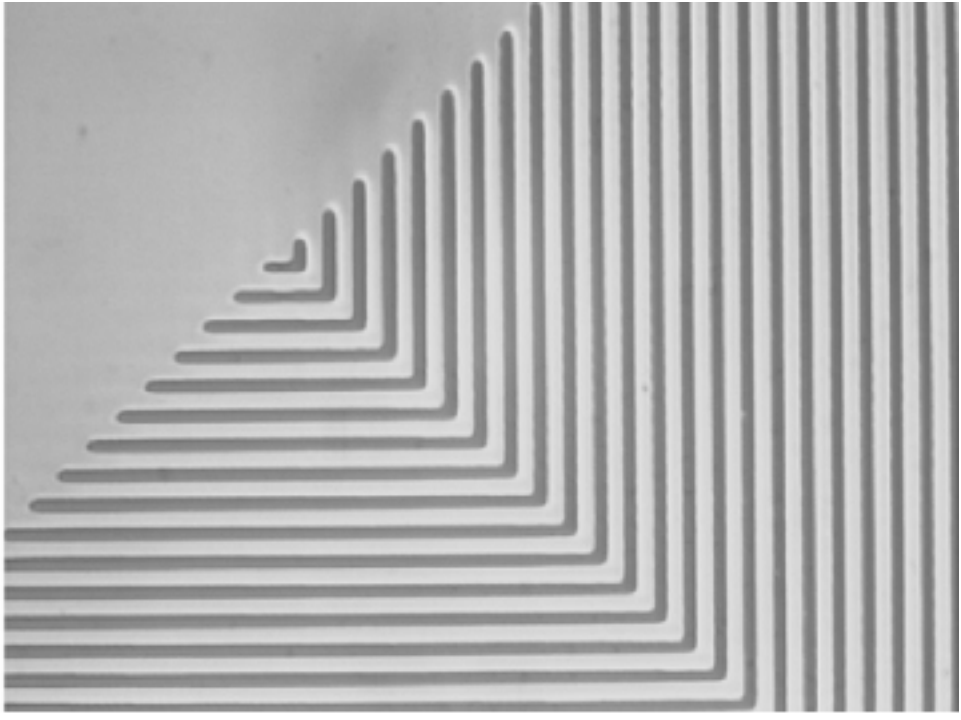

(b) With erosion

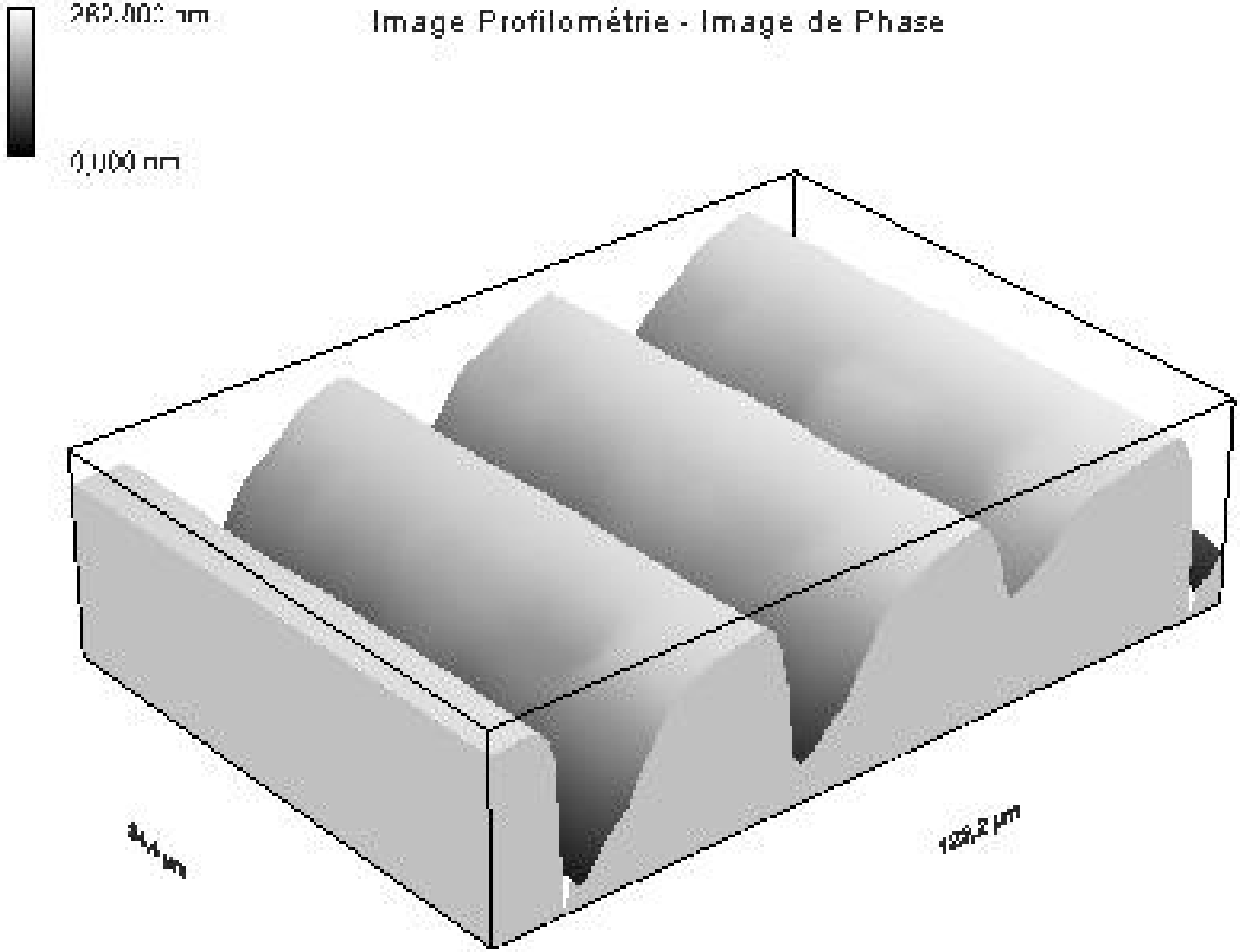

Date : 12/07/00 : 17:17:54 | Rt : 282,800 nm | Ra : 60,434 nm

Grandissement : x22,0 | Rtm : 227,400 nm | Rms : 70,028 nm

Dimension latérale : 84,4 µm × 122,2 µm

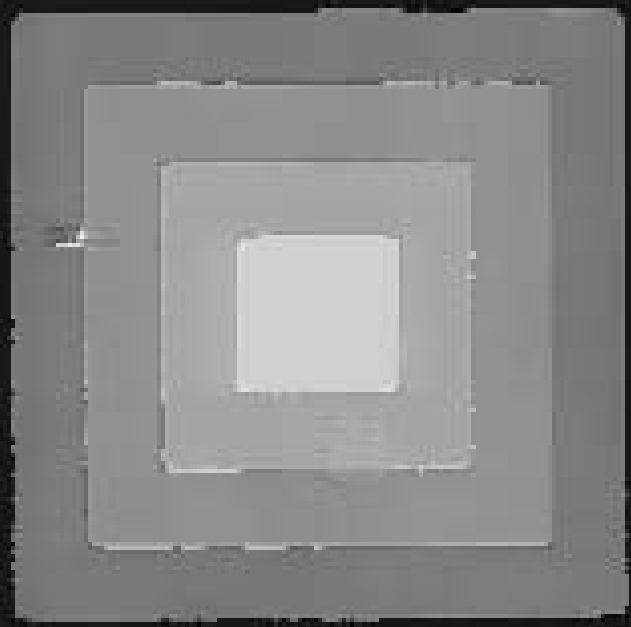

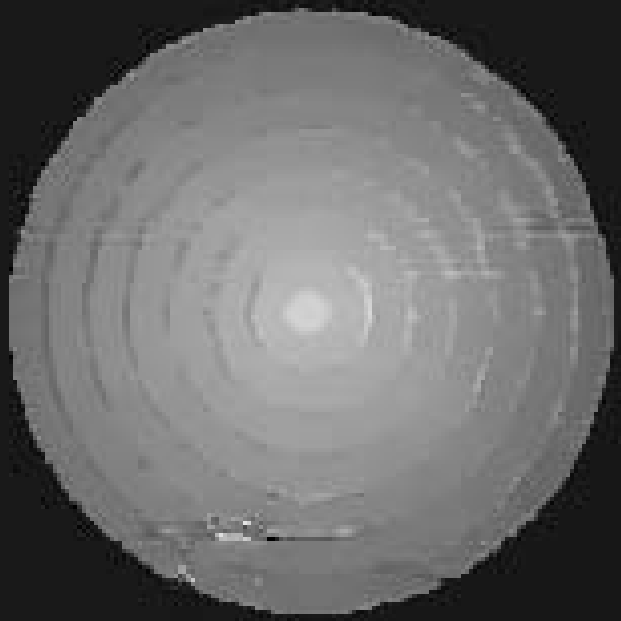

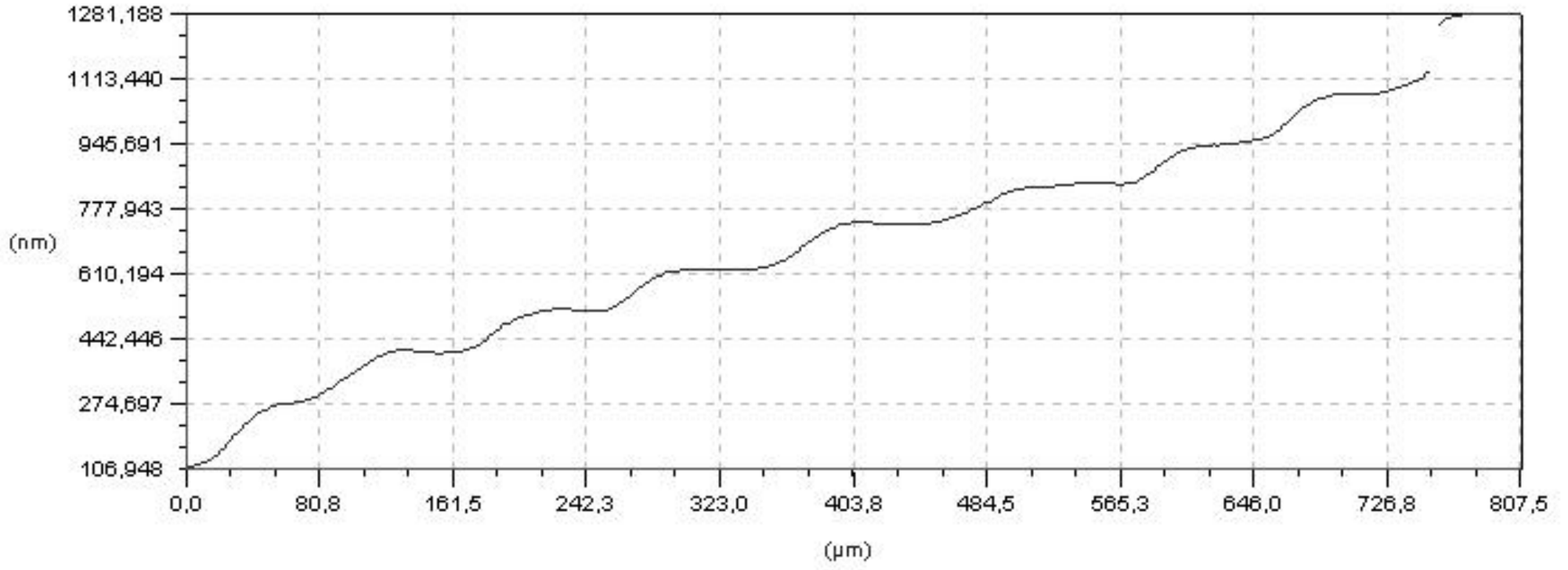

Abscisse 1: 0,0 Abscisse 2: 0,0 Ordonnée 1: 106,9 Ordonnée 2: 0,0 Delta X: 0,0 Delta Y: 106,9

Surface_1 FLOAT (78,1, 492,9)-(885,7, 541,0) - µm x nm - Rt : 1174,240 - Ra : 244,290 - Rq : 294,999 - Dimension : 809,5